MODELING GROWTH IN NEURONAL CELL CULTURES: NETWORK PROPERTIES IN DIFFERENT PHASES OF GROWTH STUDIED USING TWO GROWTH SIMULATORS

T. Mäki-Marttunen[1,2], R. Havela[1]*, J. Aćimović[1], H. Teppola[1], K. Ruohonen[2], and M.-L. Linne[1]*

[1] Department of Signal Processing, Tampere University of Technology,
[2]Department of Mathematics, Tampere University of Technology,
P.O. Box 553, FI-33101 Tampere, Finland

tuomo.maki-marttunen@tut.fi, riikka.havela@tut.fi, jugoslava.acimovic@tut.fi,
heidi.teppola@tut.fi, keijo.ruohonen@tut.fi, marja-leena.linne@tut.fi

ABSTRACT

In this work we study the structural changes in neuronal networks emerging during network maturation. We analyze two computational models proposed in the literature that describe the growth of neurons. The models have planar geometry and the density of cells is chosen to correspond to the 'dense' and 'sparse' cultures reported in the experimental studies. The growth of the model neurons and networks is simulated using two novel publicly available simulators. A graph representation of the networks is obtained from the simulation results and examined at days 7, 14, and 21. The two models are clearly different in nature. The first can model large networks phenomenologically, while the second describes some of the relevant biophysical processes in smaller networks. The difference in modeling approach is evident in the graph properties.

1. INTRODUCTION

Network models of interconnected neurons have been extensively studied in the past to assess the mechanisms of information transmission and processing in different brain regions. Majority of these studies focus on the models of mature cortical circuits. The model neurons are described by dynamics of the cell membrane potential, including various contributing mechanisms at different levels of complexity. The networks have stable topology based on experimental observations. The contacts between neurons, the synapses, are activity-dependent.

The structural properties of the network topology impose limitations to the overall functionality. In this work, we focus on the analysis of realistic topologies without explicitly considering the activity and function of the corresponding networks. Instead, the goal is to examine the structural changes emerging during realistic simulations of growth of neurons and neuronal networks.

Growth models reported in the literature often focus on a single neuron or a single neurite, describing the underlying biophysical processes. For example, the models of initiation, elongation, and retraction of neurites, sensitivity to extracellular chemicals, selection of growth direction, and branching are reviewed in [1]. In addition, the phenomenological models of growth based on the statistical description of these processes and obtained experimentally are studied in [2], [3]. A network level model focusing on axon growth, particularly on selection of growth direction based on extracellular cues, is proposed in [4]. Recently, two simulators of neuronal growth were proposed in [3] and [5]. First of them employs statistical approach from [2]. It allows simulation of large networks with an approximative description of growth. The second simulator includes a detailed description of neurons and extracellular space, but cannot simulate large networks. We analyze the generic model from [5], but the implementation of new models is also supported.

The relevant aspects of growth greatly depend on the considered experimental conditions. We focus on *neuronal cell cultures* which allow monitoring of growth for several months, and inspection of the structural changes at least during the first weeks. Staining and microscopy techniques provide the tools for monitoring the structural changes. Various parameters like initial cell density and environmental chemicals can be easily controlled.

We study the two models proposed in [3] and [5]. In order to model neuronal cultures, the planar geometry is imposed as well as the several biophysical parameters defining the neuron behavior. The presented results correspond to the days 7, 14, and 21 *in vitro*. A directed graph capturing the network connectivity pattern is extracted, and various structural measures are computed according to [6], [7]. The network activity is not explicitly considered in any of the models, so the obtained synapses correspond to the 'potential synapses', i.e. the places where a contact between two neurons *can* be established in the presence of activity. According to [8], only a fraction of these 'potential synapses' become functional synapses, which is taken into account when examining the connectivity.

*** The first two authors equally contributed to this paper.**

2. MATERIALS AND METHODS

We analyze the two recently published simulators of neuronal growth and their generic models corresponding to neuronal cell cultures described in [3], [5]. The model implemented in NETMORPH focuses on statistical description of elongation, branching, and selection of growth direction [2]. The interaction between neurons, and the role of extracellular substances are not considered. The second simulator, CX3D, allows free selection of the model with many biophysical details included [5]. We adopt the generic model for neuronal cell cultures. It includes interaction between neurons through extracellular space. Cells diffuse guidance cues into the extracellular space and the branching and direction selection of their neighbors depends on the concentration of these cues.

2.1. NETMORPH simulator for modeling network growth phenomenologically

The NETMORPH is a neuronal growth simulator for generating large-scale networks with realistic morphologies [3]. The simulator allows neurons to grow axons and dendrites but not to divide or to evoke movement. Synapses are formed when axons and dendrites come close enough to each other. The growth of the neurites includes elongation, branching, and the choice of growth direction.

The elongation of a terminal segment of a neurite is described in [3], [2] as

$$\nu(t) = \nu_0 n(t)^{-F}.$$

Here, $\nu(t)$ represents the average elongation rate of a terminal segment at time t, ν_0 is a constant, $n(t)$ is the number of terminal segments in the neuron, and F is a constant parameter determining the level of competition for resources between terminal segments. The branching process is defined in [3], [2] by the probability of a terminal segment j branching at time step $(t_i, t_i + \Delta t)$ into two new terminal segments as follows

$$p_{i,j} = n_i^{-E} B_\infty e^{-t_i/\tau}(e^{\Delta t/\tau} - 1)2^{-S\gamma_j}/C_{n_i}.$$

Here, n_i is the number of terminal segments in the whole cell at time t_i, E is a constant determining the magnitude of competition, and B_∞ and τ are constant parameters governing the intensity and slowness of the branching. The variable γ_j is the centrifugal order of the terminal segment j, i.e. the number of segments between the soma and the terminal segment, S is a constant that determines the effect of the centrifugal order on the branching rate, and $C_{n_i} = \frac{1}{n_i}\sum_{k=1}^{n_i} 2^{-S\gamma_k}$ is a normalization constant.

Neurites can change growth direction, and the probability of the change at time $t + \Delta t$ depends on the increase in length of the terminal segment during the time interval $(t, t + \Delta t)$. The new direction depends on the previous growth directions for the considered neurite segment.

The above-mentioned models are used with the following parameters. Axon growth: $F = 0.16$, $\nu_0 = 45\ \mu$m/day, $B_\infty = 17.38$, $E = 0.39$, $S = 0$, $\tau = 14$ days, dendrite growth: $F = 0.39$, $\nu_0 = 12\ \mu$m/day, $B_\infty = 4.75$, $E = 0.39$, $S = 0$, $\tau = 3.7$ days. In the synapse formation a filling fraction of $1/4$ is used, i.e. only one quarter of potential synapses are accepted as functional synapses. For other parameters the default values of the NETMORPH simulator are assigned. Simulation time step is set to 2.4 hours.

2.2. CX3D simulator for modeling network growth biophysically

The CX3D is a simulation package suitable for modeling biophysical processes related to growth of neurons. Both intracellular and extracellular processes can be taken into account. The user can specify which processes should be included and at what level of complexity. We study the model of neuronal cell cultures proposed for this simulator in [5].

A fixed number of neurons is randomly distributed in the planar space that corresponds to the cell culture. No cell division or death can occur. All cells secrete a substance which acts as a guidance cue attracting the neurites of other cells. This is the only chemical implemented in the model. A number of initial neurite segments are placed on each cell. Neurite elongation occurs with a fixed rate that is adopted from NETMORPH, i.e. $\nu = 12\ \mu$m/day for dendrites and $\nu = 45\ \mu$m/day for axons. Neurite branching, the splitting of the neurite tip into the two new segments, occurs with a certain probability if the concentration of the guidance cue is large enough. During elongation dendrites gradually become thinner, losing 0.1% of their diameter in each time step, and branching stops when a certain threshold in the diameter is reached. Extracellular gradients of the guidance cue determine the direction of growth of neurites. When the concentration of guidance cue is small the neurites will grow straight. Mechanical tensions between soma and neurites, present during elongation, retraction and branching, are included in the model as described in [5]. The filling fraction and the simulation time step are equal to ones used in NETMORPH.

2.3. Characterization of network properties

The simulated networks are converted into unweighted directed graphs and analyzed using the following graph properties: degree distribution, geodesic path length, clustering coefficient, and motifs. Neurons represent graph nodes and the functional synapses form the edges. The edges are considered unweighted. Multiple synapses between two neurons form only one edge.

The set of nodes is denoted as $V = \{v_i\}_{i=1\ldots N}$ and the edges between them as $E = \{e_{ij}\}_{i,j=1\ldots N}$. The in-degree of a node is the number of edges arriving at the node, and the out-degree is the number of edges leaving the node. The geodesic path from node v_i to v_j is the shortest path between v_i to v_j, and the corresponding geodesic path length is the number of edges in this path or paths (there might be more than one shortest path for a pair of cells). The geodesic path length of the network is calculated by averaging over the geodesic path lengths of all connected nodes.

The local clustering coefficient of node v_i is defined as follows. Take all *neighbors* of v_i, i.e. such nodes v_j that $e_{ij}, e_{ji} \in E$, and calculate the ratio between the number of existing connections and the maximal number of possible connections. The global clustering coefficient is the average over local clustering coefficients of those nodes that have more than one neighbor. Clustering can also be assessed by analyzing *motifs* [7], [6]. All possible connections between triplets of nodes represent one of the 13 motifs (see Figure 2). The proportions of triples representing the motifs to the total number of triples tells us about the way the network is clustered.

3. RESULTS AND CONCLUSIONS

We simulated small networks of 100 neurons using both simulators, and the bigger networks of 10000 neurons using NETMORPH only. The cell density was selected according to the experimental studies reported in the literature [9]; we studied sparse (590 neurons$/mm^2$) and dense (1600 neurons$/mm^2$) networks at days 7, 14, and 21 *in vitro* (DIV). The simulations started from random initial conditions (cell positions, number of neurites per cell), and the presented results are the average over many repetitions. The summary of the results obtained for measures described in Section 2.3 is given in Figures 1 and 2, and in Table 1. The in- and out-degree distributions are shown in Figure 1, and the frequency of motifs in Figure 2. The remaining measures are given in Table 1. For comparison, the same measures are evaluated for random networks chosen to have the same mean of the degree distribution as the simulation results.

Difference between the two models is already visible in the degree distributions in Figure 1. The NETMORPH model significantly deviates from the random network (shaded area in figures). The CX3D model differs less and the difference is bigger for the out-degree distribution and for the networks with higher overall connectivity (cultures in latter development stage). The observed difference in results is expectable considering the intrinsic properties of the models. In NETMORPH the neurites grow in random directions, without interaction between the cells. Connections are formed when dendrite-axon pairs become close enough, which depends on several model parameters and on the initial conditions. In the CX3D model cell interaction is implemented through guidance cues secreted from the cells. The neurites are more likely to grow toward higher concentrations of guidance cues. This way, the neurons have tendency to strongly connect to the neighbors with less variability than in NETMORPH. Due to the small network size this clustering effect is not emphasized since all the neurons are close enough to form connections. The majority of results in motifs analysis significantly differ from the random values (U-test, confidence level 0.05). The rare similar values are marked with 'o' in Figure 2. In the NETMORPH model the increase in number of motifs with 'loops' between pairs of cells, most of all the number of motifs 12, happens between days 14 and 21. In addition to the two small scale models, in Table 1 are shown results for a larger model (10000 neurons) simulated in NETMORPH. There is a visible increase in the shortest path length, as a result of the overall network size. The clustering coefficient remains similar to the one in smaller networks.

In summary, the two neuronal growth models from the literature were compared to each other and to the random networks. The obtained results are significantly different, and different from random networks. More detailed analysis focused on particular aspects of neuronal growth will be carried out in the future.

4. ACKNOWLEDGMENTS

The authors would like to acknowledge the following funding: TISE graduate school, Academy of Finland project grants no. 106030, no. 124615, and no. 132877, and Academy of Finland project no. 320071 (Center of Excellence in Signal Processing).

5. REFERENCES

[1] B. Graham and A. van Ooyen, "Mathematical modeling and numerical simulation of the morphological development of neurons," *BMC Neuroscience*, vol. 7, no. Suppl 1, pp. S9, 2006.

[2] J. van Pelt and H. Uylings, *Natural Variability in the Geometry of the Dendritic Branching Patterns*, Taylor & Francis, Boca Raton, Florida, USA, 2005.

[3] R. Koene, B. Tijms, P. van Hees, F. Postma, A. de Ridder, G. Ramakers, J. van Pelt, and A. van Ooyen, "Netmorph: A framework for the stochastic generation of large scale neuronal networks with realistic neuron morphologies," *Neuroinform*, vol. 7, pp. 195–210, 2009.

[4] R. Segev and E. Ben-Jacob, "Generic modeling of chemotactic based self-wiring of neural networks," *Neural Networks*, vol. 13, pp. 185–199, 2000.

[5] F. Zubler and R. Douglas, "A framework for modeling the growth and development of neurons and networks," *Frontiers in Computational Neuroscience*, vol. 3, no. 25, 2009.

[6] R. Milo, S. Shen-Orr, S. Itzkovitz, N. Kashtan, D. Chklovskii, and U. Alon, "Network motifs: Simple building blocks of complex networks," *Science*, vol. 298, pp. 824–827, October 2002.

[7] S. Boccaletti, V. Latora, Y. Moreno, M. Chavez, and D.-U. Hwang, "Complex networks: Structure and dynamics," *Physics Reports*, vol. 424, pp. 175–308, 2006.

[8] A. Stepanyants and D. Chklovskii, "Neurogeometry and potential synaptic connectivity," *TRENDS Neurosci*, vol. 28, no. 7, pp. 387–394, July 2006.

[9] D. A. Wagenaar, J. Pine, and S. Potter, "An extremely rich repertoire of bursting patterns during the development of cortical cultures," *BMC Neuroscience*, vol. 7, no. 1, pp. 11, 2006.

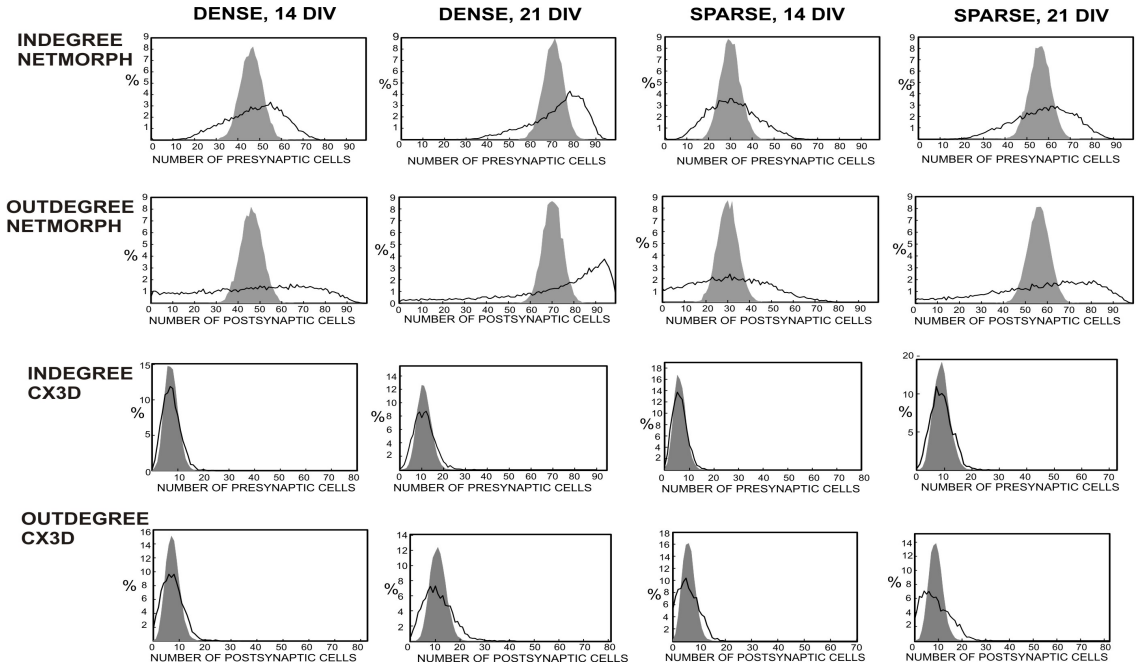

Figure 1. **In-degree and out-degree distribution.** Upper rows - degree distributions obtained using NETMORPH; bottom rows - CX3D results. Left columns - dense cultures, 14 and 21 DIV. Right columns - sparse cultures, 14 an 21 DIV. The x axis - the number of presynaptic (for in-degree) and postsynaptic (for out-degree) neurons. The y axis - degree probability (in %).

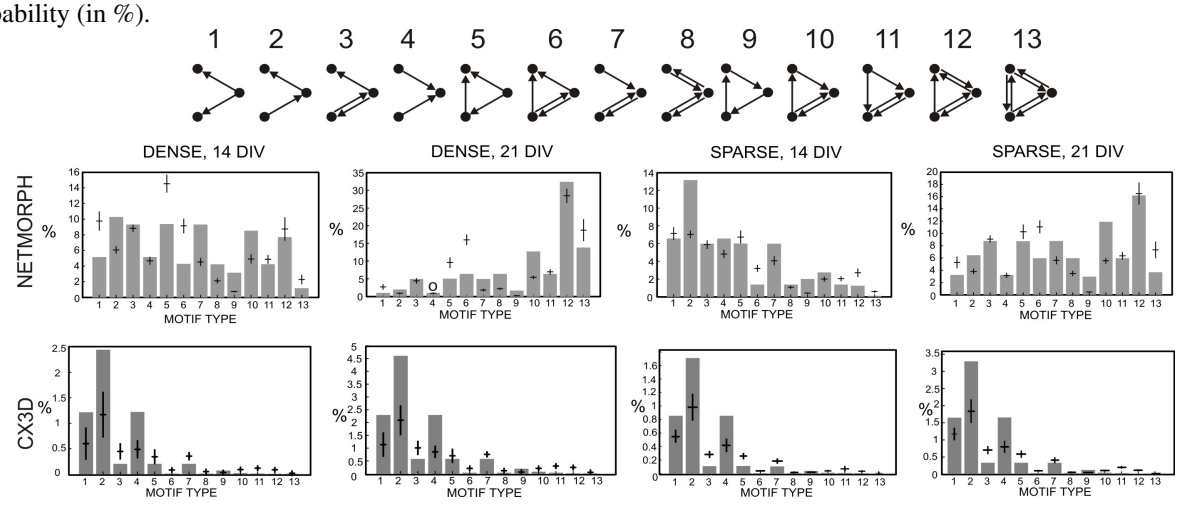

Figure 2. **Distribution of motifs** - sparse and dense networks, 14 and 21 DIV, two simulators. Gray - random networks, the results from simulated models are marked with '+', vertical arm representing the ST deviation. 'o' - not significantly different from random networks (U-test, confidence level 0.05).

		SPARSE		DENSE	
		Geodesic	Clustering	Geodesic	Clustering
CX3D SMALL	7DIV	5.1 ± 1	–	5.5 ± 1	0.3 ± 0.1
	14DIV	3.3 ± 0.3	0.5 ± 0.08	3.2 ± 0.2	0.5 ± 0.04
	21DIV	2.7 ± 0.1	0.5 ± 0.06	2.6 ± 0.1	0.6 ± 0.03
NETMORPH SMALL	7DIV	3.1 ± 1.2	0.3 ± 0.3	2.3 ± 0.8	0.3 ± 0.2
	14DIV	1.8 ± 0.6	0.6 ± 0.1	1.5 ± 0.5	0.7 ± 0.08
	21DIV	1.4 ± 0.5	0.7 ± 0.06	1.3 ± 0.5	0.8 ± 0.04
NETMORPH LARGE	7DIV	12.8 ± 5.2	0.3 ± 0.3		
	14DIV	6.7 ± 3.2	0.5 ± 0.09		
	21DIV	4.5 ± 2.3	0.6 ± 0.06		

Table 1. Computed measures (mean $\pm$ standard deviation). Each row corresponds one of two simulators, one time point, and small (100 cells) or large (10000 cells) networks. All results are significantly different from the random network.